Solids modeled by ab initio crystal field methods. Part 16: An ab initio study of the geometry of 2-(2-methyl-3-chloroanilino) nicotinic acid: gas phase and solid state calculation...

ARTICLE *in* ELECTRONIC JOURNAL OF THEORETICAL CHEMISTRY · JANUARY 1997

DOI: 10.1002/ejtc.50

4 AUTHORS, INCLUDING:

Christian Van Alsenoy
University of Antwerp
403 PUBLICATIONS **5,927** CITATIONS

SEE PROFILE

Solids modeled by *ab initio* crystal field methods. Part 16: an *ab initio* study of the geometry of 2-(2-methyl-3-chloroanilino) nicotinic acid: gas phase and solid state calculations

K. FRANCKAERTS, A. PEETERS, A. T. H. LENSTRA AND C. VAN ALSENOY*

University of Antwerp (UIA), Department of Chemistry, Universiteitsplein 1, B-2610 Wilrijk, Belgium

ABSTRACT

The geometry of 2-(2-methyl-3-chloroanilino)nicotinic acid was studied in the gas phase and in the solid state using *ab initio* Hartree–Fock methods. Three different conformers were found in the gas phase. The structures of two polymorphic forms were optimized in a crystalline environment modeled by point charges. The calculations were carried out using the 6-31G basis set for the H, C, N and O atoms and the 6-6-31G basis set for the Cl atom. The MIA method was used in the SCF procedure of all calculations. ©1997 by John Wiley & Sons, Ltd.

Received 10 April 1997; Accepted 29 April 1997

Electron. J. Theor. Chem., Vol. **2**, 168–179 (1997)

No. of Figures: 3 No. of Tables: 7 No. of References: 13

KEY WORDS 2-(2-methyl-3-chloroanilino)nicotinic acid; polymorphism; solid state; *ab initio* SCF; MIA method; cluster model; point charge model; image/mirror-image dimer

INTRODUCTION

In the solid state 2-(2-methyl-3-chloroanilino)nicotinic acid (NIC) exhibits conformational polymorphism. This phenomenon in which various crystal structures have different conformations, occurs frequently in complex compounds, especially in molecules where hydrogen bond formation is possible [1].

In the past, four different forms of NIC could be crystallized from ethyl acetate, methanol, ethanol and acetone solutions respectively [2]. Several experimental tools like thermoanalysis, UV spectroscopy, IR spectroscopy and X-ray diffraction were used for the characterization of these crystals and they indeed confirmed the existence of four different polymorphic forms denoted NIC-I, NIC-II, NIC-III and NIC-IV [2].

NIC-I crystallizes in the monoclinic space group $C2_1/c$ with four molecules in the unit cell, NIC-II crystallizes in the orthorhombic space group $Pca2_1$ with four molecules per unit cell, while NIC-III and NIC-IV crystallize in the triclinic space group $P-1$ containing two molecules in each unit cell [2].

This report describes a theoretical study of the different molecular conformations. *Ab initio* SCF optimizations were performed for NIC in the gas phase as well as in the different crystal structures. The experimental X-ray conformations [2] were used as an initial guess for the geometry optimizations.

*Correspondence to: C. Van Alsenoy.

CCC 1082–4928/97/010168–12$17.50

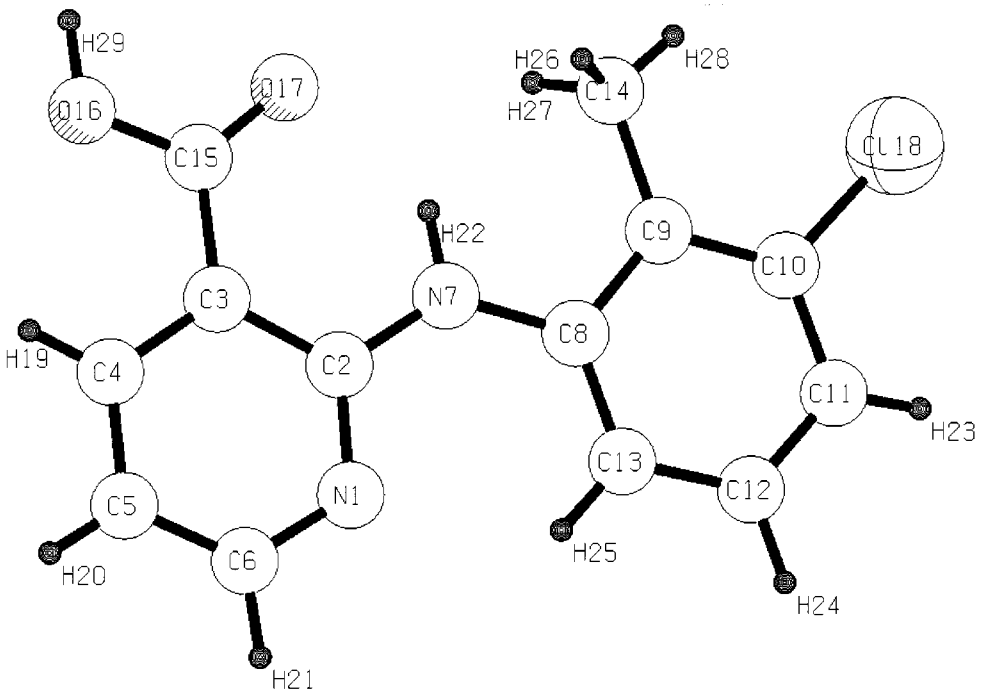

Figure 1. Atom numbering

In the study of the solid state, the cluster model has been used [3]. In this model, a molecule is surrounded by other molecules, geometrically arranged in accordance with space group symmetry. There are two important variations of the cluster model: the point charge model (PC) [4] in which the central molecule and the neighboring molecules interact purely electrostatically and the more advanced super molecule model (SM) [5] in which a group of several molecules is treated quantum mechanically while the rest of the environment is treated electrostatically. When the overlap between the central molecule and the nearest neighbors is negligible, the PC model is sufficient for the description of the system, otherwise the SM model is preferred.

Because the structure of NIC is too large for SM calculations, only the PC model could be used in order to simulate a crystalline environment. Recently the PC model has been applied in a study of sulfapyridine (SP) [6], a compound comparable in size to NIC that also exhibits conformational polymorphism. Because theoretical results for the SP polymorphs were in good agreement with the experimental results, it was decided to apply the PC model to model the crystal structures of NIC.

The atom numbering used is shown in Figure 1. Arabian and Roman numerals are used to denote the gas phase and crystal structures respectively. In Tables 1–4, the *ab initio* results for the gas phase conformations are summarized. In Tables 5–7, the X-ray data and *ab initio* results for the PC model of the polymorphs NIC-III and NIC-IV respectively, are presented.

COMPUTATIONAL PROCEDURES

Geometry optimizations were started from the X-ray experimental atomic positions [2]. Use of the 6-31G basis set for the atoms O, N, C and H [7] and the 6-6-31G basis set for Cl [8] results in a total

of 188 contracted Gaussians for the description of a conformer.

In the solid state calculations, the neighboring molecules were represented by point charges (PC) fixed on atomic positions, generated in accordance with the space group, experimental cell parameters and symmetry operations obtained from an X-ray experiment [2]. Cell parameters, symmetry operations as well as the orientation of the central entity in the crystalline environment, were kept constant during the optimizations. Atomic point charges were extracted from the molecular wave function via a stockholder type analysis [9]. Stockholder charges are obtained by dividing the molecular density in a given point between all the atoms of the molecule in proportion to the pure atomic densities in that point.

The crystalline environment has been determined by surrounding every atom of the central molecule by an imaginary sphere of 20 Å radius. All the neighboring molecules with at least one atom within the volume defined by the union of these spheres were included in the model. The resulting model contained approximately 250 to 280 neighboring molecules for the different polymorphs.

For the gas phase as well as the solid state, complete geometry optimizations were performed using the program BRABO [10]. For the SCF calculations, the MIA approach [11] was used, a combination of direct SCF [12] and the multiplicative integral approximation. This method is extremely useful to study very large systems and allows very fast SCF calculation by reducing the number of integrals to be calculated in each iteration without losing accuracy with respect to a conventional approach. For the calculation of the forces on the atoms, the standard gradient method [13] as implemented in BRABO was used. For the optimization modeling the solid state, only forces on atoms of the 'central' molecule need to be calculated as only this molecule is representative for a molecule in a crystalline environment. This procedure reduces to a large extent the CPU time needed for a gradient evaluation.

All the structures were refined until all the Cartesian forces were smaller than the usual threshold of 0.001 mdyne. At this level of refinement, internal parameters are supposed to be converged to 0.0002 Å for bond lengths and to 0.1° for angles.

RESULTS AND DISCUSSION

Gas phase

Three different structures were optimized in the gas phase for NIC: two neutral forms denoted NIC-1 and NIC-2, and one zwitterionic form denoted NIC-Z.

In the zwitterionic form NIC-Z the hydrogen atom H_{29} is bonded to the N_1 atom of the pyridine ring, whereas in all the neutral forms the H_{29} atom is attached to the carboxyl group. Thus NIC-Z is characterized by a positively charged N_1 atom and a negatively charged carboxylate group and is therefore a zwitterion.

The common feature of all the gas phase conformers is that the pyridine ring, the carboxyl group and the N_7 and C_8 atoms form an almost planar system, whereas the substituted benzene ring is twisted from this plane. Because the angle between the two six-membered rings is reflected by the torsions around the C_8–N_7 bond, the rotation potential around the C_8–N_7 bond has been calculated for both the neutral and zwitterionic forms. In these calculations, the torsion potential involved the enumeration of the energy in function of the C_9–C_8–N_7–C_2 torsion angle while refining all other parameters. The potential curve for the neutral NIC structure is presented in Figure 2 whereas the potential curve for the zwitterionic form is given in Figure 3. The relative energies of the different conformers obtained by rotating about the C_8–N_7 bond are presented in Table 1.

For the neutral form (Figure 2), there are four minima, which are two by two identical because of symmetry. The respective minima are located at a C_9–C_8–N_7–C_2 torsion angle of 75.7° for the image and 284.3° for the mirror-image, and at a C_9–C_8–N_7–C_2 torsion angle of 137.4° for the image

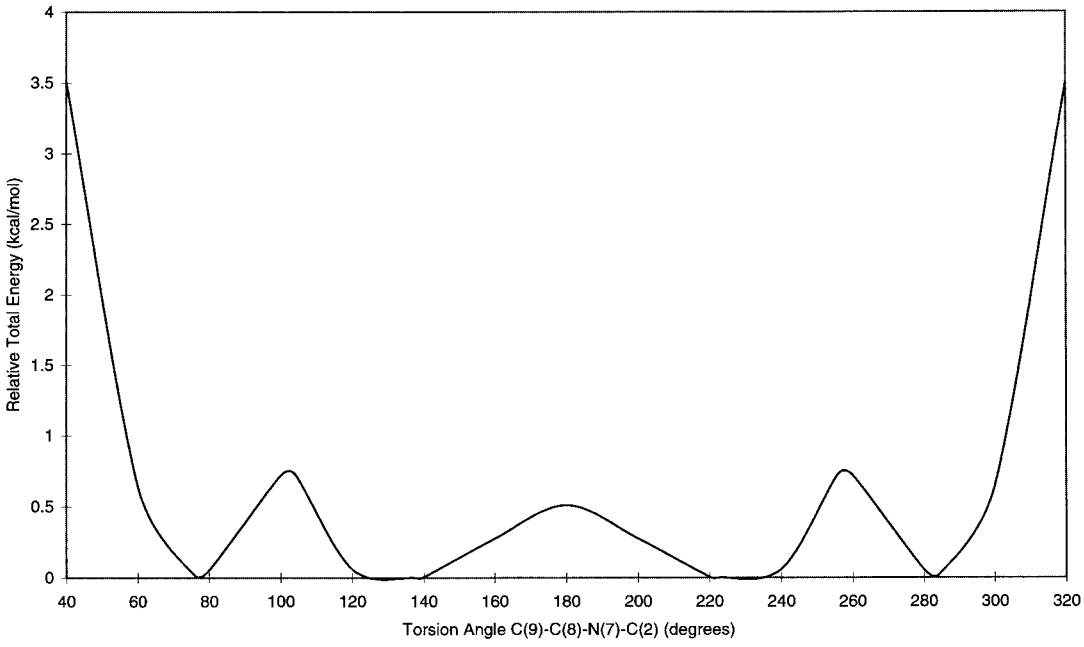

Figure 2. Neutral form

Table 1. The relative total energy (E_r, in kcal mol^{-1}) as a function of the C_9–C_8–N_7–C_2 torsion angle (ϕ_t, in degrees)

Torsion angle ϕ_t	Neutral form E_r	Zwitterionic form E_r
0.00	15.117 (MAX)	22.515 (MAX)
20.00	8.102	9.220
40.00	3.507	4.498
60.00	0.642	1.590
75.72	0.021 (NIC-1)	–
80.00	0.055	0.571
100.00	0.720	0.105
104.04	0.729 (MAX)	–
110.50	–	0.000 (NIC-Z)
120.00	0.059	0.098
137.36	0.000 (NIC-2)	–
140.00	0.004	1.103
160.00	0.275	3.356
180.00	0.509 (MAX)	8.708 (MAX)

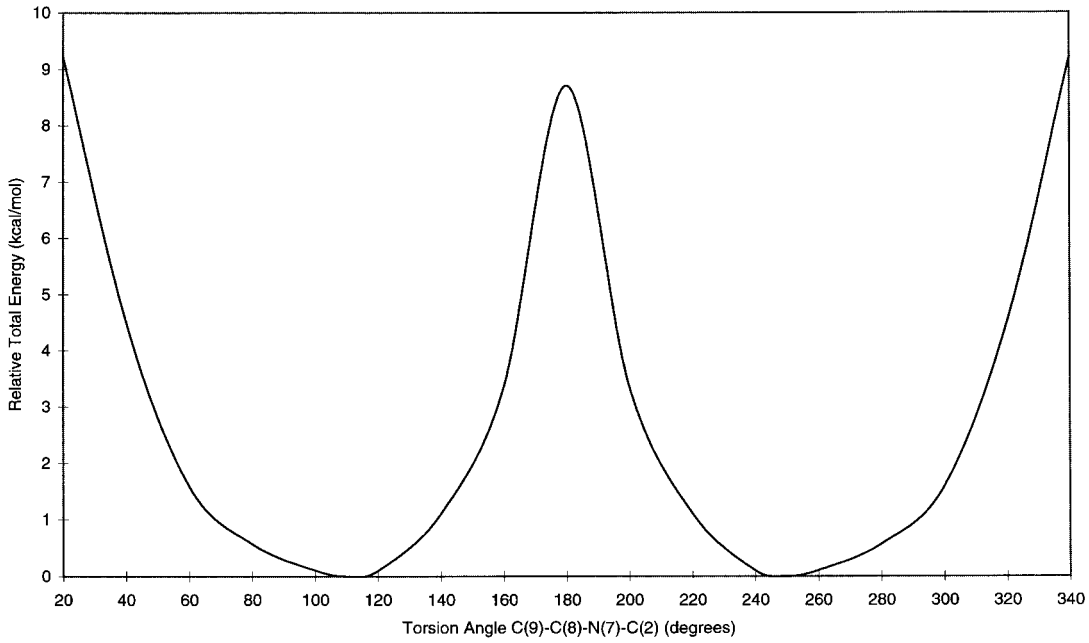

Figure 3. Zwitterionic form

and 222.6° for the mirror-image. The 0° torsion angle conformer corresponds to a very high energy maximum (15.12 kcal mol^{-1}). There are two other local maxima, one located at 104.0° for the image and at 256.0° for the mirror-image (0.73kcal mol^{-1}), and one at 180.0° (0.51 kcal mol^{-1}).

For the zwitterionic form (Figure 3), two minima related by symmetry are found. They are located at a C_9–C_8–N_7-C_2 torsion angle of 110.5° for the image and 249.5° for the mirror-image. Furthermore, a very high potential barrier (22.52 kcal mol^{-1}) is situated at a 0° torsion angle, while a lower barrier (8.71 kcal mol^{-1}) is located at a 180° torsion angle.

Because the potential barriers between the conformers are very low, the NIC-1 and NIC-2 conformations can easily be transformed one another. Transformation between the image and the mirror-image conformational structure of NIC-Z requires an excitation energy of 8.71 kcal mol^{-1} and is therefore impossible. Due to the enormous steric hindrance between the two ring systems, the potential barrier situated around 180°, which exists in the neutral as well as in the zwitterionic case, is very high (15.12 kcal $mol^{-1}$and 22.52 kcal mol^{-1} respectively) and can therefore never be bridged.

The energy of the zwitterionic form NIC-Z is 21.03 kcal mol^{-1} higher than the energy of the NIC-2 conformer.

The calculated internal parameters for the NIC-1, NIC-2 and NIC-Z conformers are listed in Tables 2–4.

The neutral forms are characterized by an aromatic pyridine ring. All the C–C and C–N bonds belonging to the pyridine ring are indeed very similar, with the exception of the C_2–C_3 bond length which is larger. The mean value for the C–N bond length of all neutral forms is about 1.33 Å whereas the mean value for the C–C bond length is about 1.40 Å. The pyridine ring of NIC-Z on the other hand is less aromatic, resulting in alternating C–C distances. The differences between single and double C–C bonds belonging to the pyridine ring amounts to 0.07 Å.

Deprotonation elongates C_{15}–O_{17} and shortens C_{15}–O_{16} to such an extend that the latter has the most

Table 2. Bond lengths of the gas phase conformers NIC-1, NIC-2 and NIC-Z

	NIC-1	NIC-2	NIC-Z
C2–N1	1.3394	1.3382	1.3541
C3–C2	1.4183	1.4207	1.4291
C4–C3	1.3949	1.3944	1.3588
C5–C4	1.3804	1.3806	1.4246
C6–N1	1.3245	1.3247	1.3757
C6–C5	1.3886	1.3876	1.3454
N7–C2	1.3564	1.3583	1.3259
C8–N7	1.4257	1.4174	1.4222
C9–C8	1.4004	1.4044	1.4016
C10–C9	1.3879	1.3882	1.3895
C11–C10	1.3803	1.3796	1.3804
C12–C11	1.3836	1.3842	1.3851
C13–C8	1.3870	1.3886	1.3908
C13–C12	1.3843	1.3830	1.3841
C14–C9	1.5041	1.5085	1.5080
C15–C3	1.4550	1.4555	1.5314
O16–C15	1.3544	1.3534	1.2352
O17–C15	1.2238	1.2244	1.2746
Cl18–C10	1.8180	1.8195	1.8098

Table 3. Valence angles of the gas phase conformers NIC-1, NIC-2 and NIC-Z

	NIC-1	NIC-2	NIC-Z
C3–C2–N1	120.34	120.06	117.78
C4–C3–C2	118.01	118.09	118.55
C5–C4–C3	120.62	120.67	121.92
C6–N1–C2	120.47	120.68	123.44
C6–C5–C4	117.33	117.25	118.28
C5–C6–N1	123.23	123.25	120.03
N7–C2–N1	117.11	118.21	121.12
N7–C2–C3	122.56	121.73	121.10
C8–N7–C2	124.77	127.86	126.69
C9–C8–N7	121.16	117.55	119.25
C10–C9–C8	116.36	116.71	116.26
C11–C10–C9	123.50	123.22	123.31
C12–C11–C10	118.93	118.75	119.20
C13–C8–N7	117.79	121.47	119.41
C13–C8–C9	121.01	120.91	121.32
C13–C12–C11	119.45	120.14	119.50
C12–C13–C8	120.74	120.24	120.39
C14–C9–C8	121.77	120.46	121.81
C14–C9–C10	121.87	122.83	121.92
C15–C3–C2	121.52	121.72	121.10
C15–C3–C4	120.47	120.19	120.34
O16–C15–C3	114.00	114.05	115.76
O17–C15–C3	126.01	125.99	114.41
O17–C15–O16	119.99	119.96	129.83
Cl18–C10–C9	119.71	120.34	119.51
Cl18–C10–C11	116.80	116.43	117.18

Table 4. Torsion angles of the gas phase conformers NIC-1, NIC-2 and NIC-Z

	NIC-1	NIC-2	NIC-Z
C8–N7–C2–N1	3.72	−0.03	−3.13
C8–N7–C2–C3	−176.32	179.48	176.39
H22–N7–C2–N1	178.23	−178.39	−178.09
H22–N7–C2–C3	−1.91	1.12	1.43
C9–C8–N7–C2	−75.72	−137.36	−110.50
C13–C8–N7–C2	106.32	45.64	71.00
C9–C8–N7–H22	109.95	40.98	63.83
C13–C8–N7–H22	−68.02	−136.02	−114.67
H26–C14–C9–C8	103.35	37.31	−127.59
H26–C14–C9–C10	−76.45	−143.31	51.71
H27–C14–C9–C8	−16.45	−82.36	113.62
H27–C14–C9–C10	163.90	97.03	−67.09
H28–C14–C9–C8	−136.90	157.67	−7.61
H28–C14–C9–C10	43.30	−22.94	171.68
O16–C15–C3–C2	−179.53	178.75	178.73
O16–C15–C3–C4	0.82	−1.82	−2.71
O17–C15–C3–C2	0.58	−1.43	−1.90
O17–C15–C3–C4	−179.07	178.00	176.60
H29–O16–C15–C3	−179.95	179.78	–
H29–O16–C15–O17	−0.05	−0.05	–

double bond character. Differences in bond lengths decrease from 0.13 Å in the neutral forms to 0.04 Å in the zwitterionic form. The elongation of C_{15}–O_{17} and the enlargement of the valence angle in NIC-Z can be explained by the very strong hydrogen bond between O_{17} of this carboxylate group and the H_{22} atom. This intramolecular hydrogen bond, which is present in all conformations, is strongest in NIC-Z and becomes weaker in NIC-2 and NIC-1. The distance between O_{17} and H_{22} is 1.577, 1.926 and 1.967 Å for the conformers NIC-Z, NIC-2 and NIC-1 respectively.

Examining Table 4 we find that rotation around the C_8–N_7 bond has also led to a change in the orientation of the methyl group, reflected by varying torsion angles around the C_9–C_{14} bond. For example, the H_{26}–C_{14}–C_9–C_8 torsion angle has respective values of 103.3, 37.3 and −127.6° for the conformers NIC-1, NIC-2 and NIC-Z.

Crystal phase

Four different polymorphic forms have been observed experimentally for NIC. One of these, NIC-II is a zwitterionic form whereas the other forms were found to be unionized. Conformational differences between the four crystal structures are caused by the differences of the torsion around the C_8–N_7 bond. Furthermore in all polymorphs, an intramolecular hydrogen bond is observed between the H_{22} atom and the O_{17} atom of the carboxyl group on the pyridine ring. This intramolecular H bond was found to be shortest in the NIC-II polymorph (1.754 Å). Also different types of intermolecular hydrogen bonds were detected in the experimentally observed crystals of NIC. In form I an intermolecular H bond is found between the N_1 atom of the pyridine ring and the H_{29} atom of the carboxyl group (1.610 Å). In forms III and IV mutual intermolecular H bonds are observed between the oxygens and hydrogens of each carboxyl group (1.703 and 1.738 Å respectively), while in form II an intermolecular H bond is seen between the negatively charged oxygen atom O_{16} of the carboxylate group and the hydrogen atom H_{29} on the N_1 atom of the pyridine ring (1.821 Å).

Polymorphs I and II

Refinement of the crystal structures NIC-I and NIC-II did not lead to stable minima because certain intermolecular distances became unreasonably small during the refinement procedure. The stockholder charges failed to simulate the true field which the molecules feel in a crystalline environment leading to the conclusion that the PC model is inadequate to describe these polymorphs.

Polymorph III

The experimental and calculated internal parameters of the polymorphic form NIC-III are listed in Tables 5–7.

The largest deviations between calculated and experimental bond lengths are found for the C_{15}–O_{16} bond and the C_{10}–Cl_{18} bond. The calculated C_{15}–O_{16} bond is 0.03 Å longer than the experimental bond, resulting in a more asymmetric carboxyl group. The fact that the calculated C_{10}–Cl_{18} bond is 0.07 Å longer than the experimental bond is probably due to the limitations of the 6-6-31G basis functions used for Cl. The addition of polarization functions would give a better description for this bond.

The largest difference between theoretical and experimental valence angles for the heavy atoms is observed for the O_{16}–C_{15}–O_{17} valence angle. The theoretical angle is 2.2° smaller than the corresponding experimental value. If also the valence angles containing hydrogen atoms are considered, maximum deviations are found for the valence angles of the CH_3 group and the C_{15}–O_{16}–H_{29} valence angle. All the theoretical H–C_{14}–H valence angles of the CH_3 group are close to the expected tetrahedral values whereas the experimental values vary between 91 and 114°. The C_{15}–O_{16}–H_{29} valence angle is enlarged from 103 to 114° during the optimization. Taken the known fact into account that standard X-ray crystallography has difficulty in determining the H positions with the same accuracy as heavy atoms, these discrepancies may be attributed to the experiment.

Table 5. Bond lengths of the experimental [2] crystal structure (EXP-III and EXP-IV) and the calculated stockholder model (CALC-III and CALC-IV) of the NIC-III and NIC-IV polymorphic form respectively

	EXP-III	CALC-III	EXP-IV	CALC-IV
C2–N1	1.3278	1.3384	1.3439	1.3363
C3–C2	1.4185	1.4271	1.4312	1.4285
C4–C3	1.3879	1.3960	1.3881	1.3974
C5–C4	1.3731	1.3868	1.3833	1.3852
C6–N1	1.3308	1.3278	1.3289	1.3267
C6–C5	1.3763	1.3850	1.3720	1.3840
N7–C2	1.3669	1.3574	1.3578	1.3589
C8–N7	1.4022	1.4110	1.4020	1.4082
C9–C8	1.4108	1.4104	1.4163	1.4126
C10–C9	1.3820	1.3840	1.3876	1.3823
C11–C10	1.3834	1.3817	1.3920	1.3815
C12–C11	1.3761	1.3815	1.3668	1.3813
C13–C8	1.3886	1.3897	1.3922	1.3908
C13–C12	1.3852	1.3861	1.3863	1.3870
C14–C9	1.5038	1.5096	1.4987	1.5085
C15–C3	1.4704	1.4721	1.4732	1.4717
O16–C15	1.3090	1.3383	1.3103	1.3389
O17–C15	1.2326	1.2362	1.2293	1.2371
Cl18–C10	1.7453	1.8200	1.7450	1.8270

Table 6. Valence angles of the experimental [2] crystal structure (EXP-III and EXP-IV) and the calculated stockholder model (CALC-III and CALC-IV) of the NIC-III and NIC-IV polymorphic form respectively

	EXP-III	CALC-III	EXP-IV	CALC-IV
C3–C2–N1	122.04	120.73	121.00	120.66
C4–C3–C2	117.45	117.19	118.20	117.16
C5–C4–C3	119.88	120.89	119.81	120.89
C6–N1–C2	118.76	120.72	118.29	120.76
C6–C5–C4	118.47	117.69	117.71	117.64
C5–C6–N1	123.36	122.77	124.96	122.89
N7–C2–N1	117.42	118.50	119.43	118.89
N7–C2–C3	120.54	120.76	129.57	120.44
C8–N7–C2	132.27	130.40	132.30	131.28
C9–C8–N7	117.17	115.60	115.34	115.17
C10–C9–C8	116.46	116.88	116.76	116.99
C11–C10–C9	123.57	123.24	123.12	123.49
C12–C11–C10	118.06	118.64	118.44	118.31
C13–C8–N7	121.42	123.61	124.08	124.33
C13–C8–C9	121.35	120.75	120.58	120.49
C13–C12–C11	121.41	120.50	121.28	120.76
C12–C13–C8	119.09	119.96	119.79	119.95
C14–C9–C8	120.36	119.61	121.15	119.57
C14–C9–C10	123.15	123.52	122.09	123.43
C15–C3–C2	123.02	122.25	122.36	122.10
C15–C3–C4	119.53	120.55	119.39	120.72
O16–C15–C3	114.54	114.99	114.83	115.56
O17–C15–C3	123.57	125.35	123.35	125.16
O17–C15–O16	121.89	119.66	121.82	119.27
Cl18–C10–C9	119.84	120.79	120.18	120.55
Cl18–C10–C11	116.57	115.97	116.70	115.96

Table 7. Torsion angles of the experimental [2] crystal structure (EXP-III and EXP-IV) and the calculated stockholder model (CALC-III and CALC-IV) of the NIC-III and NIC-IV polymorphic form respectively

	EXP-III	CALC-III	EXP-IV	CALC-IV
C8–N7–C2–N1	−0.70	5.98	1.14	−6.96
C8–N7–C2–C3	178.49	−173.14	−178.76	172.48
H22–N7–C2–N1	171.41	−179.18	−179.45	178.09
H22–N7–C2–C3	−9.41	1.69	0.65	−2.46
C9–C8–N7–C2	160.24	148.82	178.81	−158.29
C13–C8–N7–C2	−22.23	−33.46	0.60	22.74
C9–C8–N7–H22	−11.60	−25.95	−0.59	16.56
C13–C8–N7–H22	165.94	151.77	180.00	−162.40
H26–C14–C9–C8	80.44	70.52	59.58	54.21
H26–C14–C9–C10	−97.34	−109.74	−121.15	−125.31
H27–C14–C9–C8	−55.74	−48.97	−59.27	−64.88
H27–C14–C9–C10	126.48	130.77	120.00	115.60
H28–C14–C9–C8	−176.76	−169.49	172.32	175.00
H28–C14–C9–C10	5.46	10.25	−8.41	−4.52
O16–C15–C3–C2	−176.99	179.52	−177.50	−177.83
O16–C15–C3–C4	3.82	0.71	4.98	0.28
O17–C15–C3–C2	3.33	−0.34	3.29	1.68
O17–C15–C3–C4	−175.86	−179.15	−174.23	179.79
H29–O16–C15–C3	171.51	−178.41	−173.30	179.19
H29–O16–C15–O1	−8.80	1.45	5.92	−0.36

In the experimental structure, the pyridine ring and the C_8–N_7 bond form a planar system. In the calculated structure, the torsions about the N_7–C_2 bond have been changed by about 5° with respect to the experimental structure. The largest differences between the calculated and experimental torsion angles are found for the torsion around the C_8–N_7 bond, e.g. the torsion angle C_9–C_8–N_7–C_2 has decreased from 160.2 to 148.8° during the refinement, resulting in less steric hindrance.

The shortest intramolecular H bond observed in the experimental structure is found between H_{22} and the O_{17} atom of the carboxyl group on benzene. The experimental value is 1.996 Å. This intramolecular H bond is even shorter in the calculated structure, the theoretical value being 1.901 Å. Another H bond has been detected between the H_{25} atom of the benzene ring and the N_1 atom of the pyridine ring. The calculated value is 2.376° corresponding to an experimental value of 2.274 Å.

In the experimental structure, strong mutual intermolecular H bonds were observed between the carboxyl groups of neighboring molecules. Experimental and theoretical values for these intermolecular H bonds are very similar (1.703 Å and 1.707 Å respectively). A weaker intermolecular H bond has been found between the H_{27} atom of the methyl group on benzene and the O_{17} atom of the carboxyl group on pyridine. The calculated value for this H bond is 2.175 Å whereas the experimental value is 2.647 Å.

Changes of the torsion angles are at most 11° (C_9–C_8–N_7–C_2 torsion). The conformation obtained by the stockholder model is basically the same as the experimental conformation of NIC-III. From these results, it can be concluded that the stockholder model is able to give a reasonable description of the NIC-III polymorph.

Polymorph IV

The experimental and *ab initio* results of the polymorphic form NIC-IV are given in Tables 5–7.

The largest deviations between calculated and experimental bond lengths are found for the C_{15}–O_{16} and C_{10}–Cl_{18} bonds. The calculated C_{15}–O_{16} bond is 0.03 Å longer than the experimental bond, leading to a more asymmetric carboxyl group bond as in the case of the NIC-III polymorph. The calculated C_{10}–Cl_{18} bond is 0.08 Å longer than the experimental, again a consequence of the poor basis set used for the description of the Cl atom.

Maximum deviations between theoretical and experimental valence angles are found for the C_6–N_1–C_2 and O_{16}–C_{15}–O_{17} valence angles. The theoretical C_6–N_1–C_2 angle is 2.5° larger than the experimental angle whereas the theoretical O_{16}–C_{15}–O_{17} angle is 2.5° smaller than the experimental angle. Considering also the valence angles containing hydrogen atoms, maximum deviations are found for the valence angles about the CH_3 group. All the theoretical H–C_{14}–H valence angles of the CH_3 group have a value of about 108° whereas the experimental values vary between 101 and 114°. Here again, these deviations may be caused by a poor determination of the H atoms using standard X-ray crystallography.

In the experiment, the complete structure of the NIC-IV polymorphic form is almost planar. During the optimization, rotations of approximately 6° about the C_2–N_7 bond and 22° about C_8–N_7 give rise to a highly non-planar structure.

The intramolecular bond between H_{22} and the O_{17} atom of the carboxyl group on benzene is 1.913 Å according to the experiment while it is 1.876 Å in the calculated structure. A weaker H bond has been detected between the H_{25} atom of the benzene ring and the N_1 atom of the pyridine ring. The calculated value is 2.292° whereas the experimental value is 2.248 Å.

In the experimental structure, strong mutual intermolecular H bonds were observed between the carboxyl groups of neighboring molecules. This interaction is stronger in theory than in experiment. The theoretical obtained distance is 1.657 Å whereas the corresponding experimental value is 1.739 Å.

The largest difference between the calculated and experimental torsion angles is about 20°. During the optimization the experimental planar NIC-IV structure becomes a non-planar system, which is also preferred by free NIC structures. Thus at a first sight, it seems that the stockholder charges were not able to mimic the crystalline environment for NIC-IV. However another point of view, explained in the next paragraph, can be taken.

Polymorph IV: new point of view

According to the X-ray experiment, the NIC-IV crystal structure is made up by dimers in which the two molecules are related by an inversion centre. The molecules of these dimers are identical, planar and linked by the hydrogen bonds between the carboxyl groups.

However, when the equilibrium geometry is calculated with the aid of *ab initio* methods starting from the experimental found geometry of NIC-IV, a non-planar structure is obtained with a C_9–C_8–N_7–C_2 torsion angle of $-158.3°$. Because the *ab initio* optimization was started from a planar structure, completely symmetric about the C_9–C_8–N_7–C_2 torsion angle, the calculation could equally well have led to the mirror-image molecule characterized by a C_9–C_8–N_7–C_2 torsion angle of 158.3°. Based on these theoretical results, it is very probable that we are faced with a racemic crystal. Combining this hypothesis with the experimental results means that each dimer would consist of an image and a mirror-image molecule, connected by the hydrogen bonds between the carboxyl groups. An X-ray experimental study of this structure could indeed lead to an average planar structure of the NIC molecules. This hypothesis is supported furthermore by the fact that the mean square displacements of the atoms involving the experimental structure are unacceptably large.

In order to investigate this new point of view further, it would be very interesting to calculate the torsion potential of the NIC-IV dimer in a crystalline environment. However the computational requirements for this type of calculations are beyond the scope of this paper and will be pursued in a forthcoming paper.

CONCLUSION

Three different gas phase conformations and two different polymorphic crystal forms have been completely optimized with standard gradient procedures. A potential curve for the gas phase has been calculated. Several attempts were made to optimize the polymorphs I and II in a PC environment, unfortunately without success. An SM model treatment of the crystalline environment is probably needed for the description of the polymorphic forms I and II. The agreement between the optimized PC model of the polymorph III and the corresponding experimental form is reasonable. In contrast to results of an X-ray experiment, a non-planar structure has been calculated for the crystal structure of polymorph IV. This discrepancy was rationalized in terms of an image/mirror-image dimer, compatible with experimental facts.

ACKNOWLEDGMENTS

A.P. and C.V.A. thank the FWO (Fonds voor Wetenschappelijk Onderzoek) for appointment as Research Assistant and Senior Research Associate respectively. This text presents the results of GOA-BOF-UA 96-99, project number 23.

REFERENCES

1. R. J. Mesley and E. E. Houghton, *J. Pharm. Pharmac.*, **19**, 295 (1967).
2. M. Takasuka, H. Nakai and M. Shiro, *J. Chem. Soc., Perkin Trans. 2*, 1061 (1982).
3. S. Saebø, B. Klewe and S. Samdal, *Chem. Phys. Lett.*, **97**, 499 (1983); J. G. Ángyán and B. Silvi, *J. Chem. Phys*., **86**, 6957 (1987); J. Bridet, S. Fliszár, S. Odiot and R. Pick, *Int. J. Quantum Chem*., **24**, 687 (1983); M. J. Mombourquette, J. A. Weil and P. G. Mezey, *Can. J. Chem*., **62**, 21 (1984).
4. P. Popelier, A. T. H. Lenstra, C. Van Alsenoy and H. J. Geise, *Acta Chem. Scand. A*, **42**, 539 (1988); P. Popelier, A. T. H. Lenstra, C. Van Alsenoy and H. J. Geise, *J. Am. Chem. Soc*., **111**, 5658 (1989); P. Popelier, A. T. H. Lenstra, C. Van Alsenoy and H. J. Geise, *Struct. Chem*., **2**, 3 (1991); A. T. H. Lenstra, C. Van Alsenoy, K. Verhulst and H. J. Geise, *Acta Crystallogr. B*, **50**, 96 (1994).
5. A. Peeters, C. Van Alsenoy, A. T. H. Lenstra and H. J. Geise, *Int. J. Quantum Chem*., **46**, 73 (1993); A. Peeters, C. Van Alsenoy, A. T. H. Lenstra and H. J. Geise, *J. Mol. Struct. (Theochem)*, **304**, 101 (1994); A. Peeters, C. Van Alsenoy, A. T. H. Lenstra and H. J. Geise, *J. Chem. Phys*., **103**, 6608 (1995).
6. K. Franckaerts, A. Peeters, C. Van Alsenoy and A. T. H. Lenstra, *Electron. J. Theor. Chem*., **2**, 96 (1997).
7. M. M. Francl, W. J. Pietro, W. J. Hehre, J. S. Binkley, M. S. Gordon, D. J. DeFees and J. A. Pople, *J. Chem. Phys.*, **77**, 3654 (1982).
8. M. S. Gordon, J. S. Binkley, J. A. Pople, W. J. Pietro and W. J. Hehre, *J. Am. Chem. Soc*., **104**, 2797 (1982).
9. F. L. Hirshfeld, *Theor. Chim. Acta*, **44**, 129 (1977).
10. C. Van Alsenoy and A. Peeters, *J. Mol. Struct. (Theochem)*, **286**, 19 (1993).
11. C. Van Alsenoy, *J. Comput. Chem*., **9**, 620 (1988).
12. M. Häser and R. Ahlrichs, *J. Comput. Chem*., **10**, 104 (1989); D. Cremer and J. Gauss, *J. Comput. Chem*., **7**, 274 (1986); J. Almlöf, K. Faegri, Jr and K. Korsell, *J. Comput. Chem*., **3**, 385 (1982).
13. P. Pulay, *Mol. Phys*., **17**, 197 (1969); P. Pulay, *Theor. Chim. Acta*, **50**, 299 (1979); P. Pulay, G. Fogarasi, F. Pang and J. E. Boggs, *J. Am. Chem. Soc*., **101**, 2550 (1997); P. Pulay, in *Advances in Chemical Physics* (ed. K. P. Lawley), Vol. LXIX, p. 241 (1987).

